Design and Structural Analysis of Novel Pharmacophores for Potent and Selective Peroxisome Proliferator-activated Receptor γ Agonists

Chia-Hui Lin,[†,‡,¶] Yi-Hui Peng,[†,||,¶] Mohane Selvaraj Coumar,[†,¶] Santhosh Kumar Chittimalla,[‡] Chun-Chen Liao,[‡,#] Ping-Chiang Lyn,[||] Chin-Chieh Huang,[†] Tzu-Wen Lien,[†] Wen-Hsing Lin,[†] John T.-A. Hsu,[†,§] Jai-Hong Cheng,[†] Xin Chen,[†] Jian-Sung Wu,[†] Yu-Sheng Chao,[†] Hwei-Jen Lee,[⊥] Chiun-Gung Juo,[∞] Su-Ying Wu,*[,†] and Hsing-Pang Hsieh*[,†]

Division of Biotechnology and Pharmaceutical Research, National Health Research Institutes, 35 Keyan Road, Zhunan Town, Miaoli County 350, Taiwan, ROC, Departments of Chemistry and Life Sciences, National Tsing Hua University, 101, Section 2, Kuang Fu Road, Hsinchu 300, Taiwan, ROC, Department of Chemistry, Chung Yuan Christian University, 200 Chung-Pei Road, Chungli 320, Taiwan, ROC, Department of Biological Science and Technology, National Chiao Tung University, Hsinchu 300, Taiwan, ROC, Department of Biochemistry, National Defense Medical Center, No.161, Section 6, Min-Chuan East Road, Taipei 114, Taiwan, ROC, and Molecular Medicine Research Center, Chang Gung University, 259 Wen-Hwa first Road, Kwei-Shan, Tao-Yuan 333, Taiwan, ROC

Received December 17, 2008

Utilizing medicinal chemistry design strategies such as benzo splitting and ring expansion, we converted PPARα/γ dual agonist **1** to selective PPARγ agonists **19** and **20**. Compounds **19** and **20** were 2- to 4-fold better than rosiglitazone at PPARγ receptor, with 80- to 100-fold PPARγ selectivity over PPARα receptor. X-ray cocrystal studies in PPARγ and modeling studies in PPARα give molecular insights for the improved PPARγ potency and selectivity for **19** when compared to **1**.

Introduction

Type 2 diabetes (T2D[a]) is one of the most common chronic diseases in developed and developing countries. T2D is characterized by fasting and postprandial hyperglycemia and relative insulin insufficiency. If left untreated, hyperglycemia and associated dyslipidemia progress to long-term macrovascular and microvascular complications such as nephropathy, neuropathy, and atherosclerosis.[1] The treatments for T2D include life style changes and use of antidiabetic medications. Despite the availability of large number of antidiabetic agents for the treatment of diabetes, WHO data show that the number of people affected from diabetes has rapidly increased from 30 million in 1985 to at least 180 million people in 2000 worldwide; this figure is likely to double by 2030.[2] This epidemic dimension of the disease necessitates the development of more effective agents for the control of diabetes and associated complications.

Peroxisome proliferator-activated receptors (PPARs) are members of nuclear hormone receptor superfamily, consisting of three subtypes, PPARα, PPARγ, and PPARδ.[3] PPARα is expressed mainly in the liver and plays a pivotal role in the uptake and oxidation of fatty acids and in lipoprotein metabolism. PPARγ is abundant in adipocytes and acts as a transcription factor regulating adipocyte differentiation and glucose homeostasis, while PPARδ is expressed in most cells and plays an important role in the regulation of lipid metabolism and cholesterol efflux.[3] Pioglitazone and rosiglitazone are two marketed PPARγ selective agonists for the treatment of diabetes, which are in clinical use since 2000. However, side effects such as heart failure, edema, fluid retention, and weight gain in patients treated with these drugs warrant development of newer drugs with better pharmacological and safety profiles.[4] In contrast to a selective PPARγ agonist, PPARα/γ dual agonist combines the insulin sensitizing potential of PPARγ agonist with the beneficial lipid modulating activities of the PPARα agonist. Thus, it was thought that a PPARα/γ dual or PPARα/γ/δ pan agonist would be an all-in-one therapy for T2D, correcting insulin resistance and lipid imbalances associated with metabolic syndrome simultaneously, and might overcome some of the side effects of a selective PPARγ agonist.[5] On the basis of this concept, several PPARα/γ-dual and PPARα/γ/δ-pan agonists were developed and tested in clinics; however, some of their developments were terminated because of concerns over cardiovascular safety in clinical trials and propensity to cause cancer in rodent models on prolonged administration. Nevertheless, development of PPAR agonists with various degrees of isoform selectivity would be helpful to better understand the biology of PPARs, as new roles and possible utilities beyond T2D for PPARs are being identified from time to time. For example, it was recently found that targeting PPARδ could be an alternative/mimic to endurance exercise in mouse models.[6] In view of these opportunities, identification of structural components controlling the selectivity for PPAR isoforms would be advantageous in designing the next generation of PPAR agonists.

In our quest to develop novel antidiabetes therapy, we have recently disclosed a series of indole based compounds for PPAR agonist activity with varying degree of selectivity toward the three isoforms of PPAR.[7−9] The design of these compounds was based on the concept that most of the known PPAR ligands have an acidic group attached to an aromatic head part, which in turn is attached to an aromatic tail part through a linker.[3] During that study, **1** with an indole head part and naphthophenone tail part was identified as PPARα/γ dual agonist (Figure 1).[8] Here, the fibrate acid group was attached to the 5-position of indole and the N-terminal was attached through a three-carbon

* To whom correspondence should be addressed. For S.-Y.W.: phone, +886-37-246-166, ext 35713; fax, +886-37-586-456; e-mail, suying@nhri.org.tw. For H.-P.H.: phone, +886-37-246-166, ext 35708; fax, +886-37-586-456; e-mail, hphsieh@nhri.org.tw.

† National Health Research Institutes.

‡ Department of Chemistry, National Tsing Hua University.

¶ These authors contributed equally to this work.

|| Department of Life Sciences, National Tsing Hua University.

Chung Yuan Christian University.

§ National Chiao Tung University.

⊥ National Defense Medical Center.

∞ Chang Gung University.

[a] Abbreviations: PDB ID, Protein Data Bank identification number; PPAR, peroxisome proliferator-activated receptor; SAR, structure−activity relationship; T2D, type 2 diabetes; TA, transactivation assay.

10.1021/jm801594x CCC: $40.75
Published on Web 03/20/2009

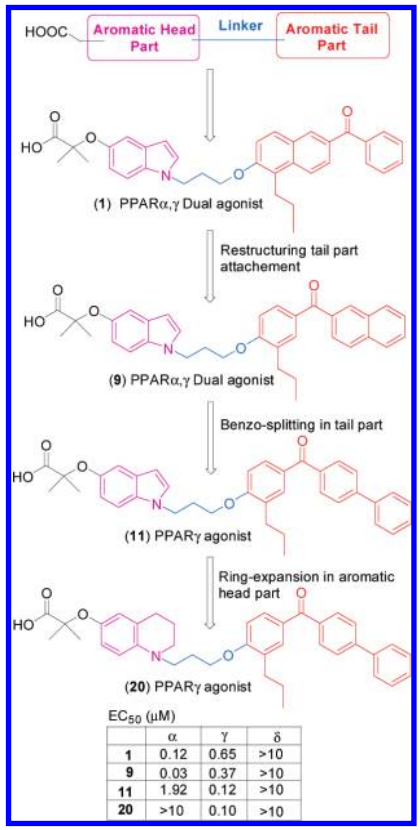

Figure 1. Identification of novel tail part building block for potent and selective PPARγ agonist activity.

Scheme 1. Synthesis of PPAR Agonists **2**−**16**[a]

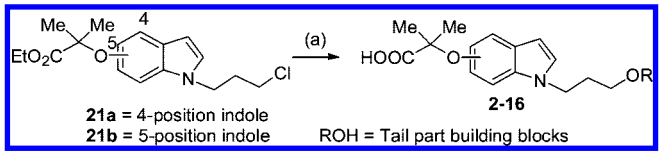

[a] (a) (i) ROH, K_2CO_3, cat. KI, DMF, 120 °C, 2 h; (ii) LiOH, MeOH/H_2O (4:1), reflux, 2 h.

linker to the tail part hydrophobic naphthophenone moiety. In continuation of our studies to develop therapeutically useful PPAR agonists with potent PPAR isoform selectivity, we have undertaken further structural modification of **1** by varying the aromatic tail part. Here we report our focused SAR exploration in the tail part which has led to the identification of 4-phenylbenzophenone as a novel tail part building block, which confers potent and selective PPARγ agonist activity in two different series of compounds. Additionally, X-ray cocrystal and molecular modeling studies of these compounds give molecular insight to the observed potency and selectivity.

Results and Discussion

Appropriately substituted indole **21**[8] was synthesized from 4-hydroxy- or 5-hydroxyindole as reported earlier and linked to the tail part building blocks employing base-induced S_N2 reaction as indicated in Scheme 1. Subsequent hydrolysis of the esters provided the required **2**−**16** (Scheme 1) with free carboxylic acid head units. For the synthesis of **17**−**20** (Scheme 2), 5- or 6-hydroxyquinoline **22** was O-alkylated with 2-bromo-2-methylpropionic acid, followed by partial hydrogenation of the quinoline ring to give **24a**,**b**. N-Alkylation of the tetrahydroquinoline ring with 1-bromo-3-chloropropane and then linking them to the appropriate tail part building blocks gave

Scheme 2. Synthesis of PPAR Agonists **17**−**20**[a]

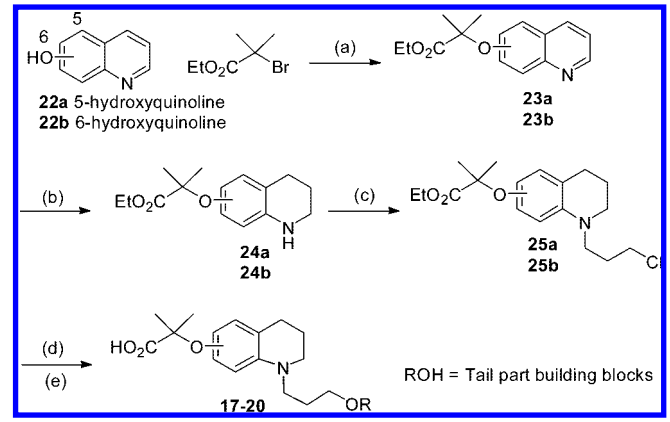

[a] (a) KOH, DMSO, room temp, 4 h; (b) $NaBH_3CN$, BF_3 ethyrate, reflux, 1 h; (c) 1-bromo-3-chloropropane, K_2CO_3, DMF, 80 °C; (d) ROH, K_2CO_3, cat. KI, DMF, 120 °C, 2 h; (e) LiOH, MeOH/H_2O (4:1), reflux, 2 h.

Table 1. PPAR Agonist Activity of Indole Analogs **1**−**16**

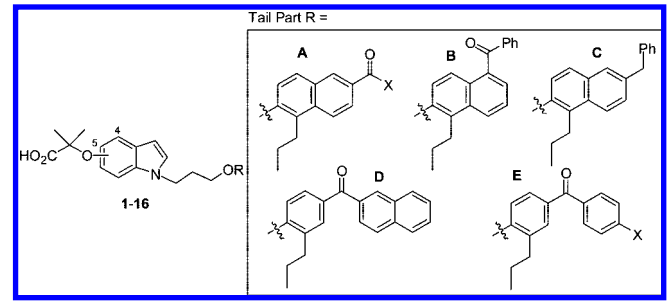

compd	indole position	tail part R	substitution X	TA EC_{50} (μM)[a] α	γ	δ
1	5	A	Ph	0.12	0.65	>10
2	5	B		0.2	3.5	>10
3	5	C		>10	>10	>10
4	5	A	CH_3	>10	1.07	>10
5	5	A	4-pyridyl	>10	2.07	>10
6	5	A	3-furanyl	0.13	0.43	>10
7	5	A	4-F-Ph	>10	2.12	>10
8	5	A	4-OCH_3-Ph	0.13	0.51	>10
9	5	D		0.03	0.37	>10
10	4	D		0.03	2.8	>10
11	5	E	Ph	1.92	0.12	>10
12	4	E	Ph	4.07	0.3	>10
13	5	E	H	0.04	0.42	5.27
14	4	E	H	0.03	>10	>10
15	5	E	F	0.13	0.9	>10
16	5	E	OCH_3	0.05	0.47	4.45
rosiglitazone				>10	0.22	>10

[a] Values are expressed as the mean of at least two independent determinations and are within ±15%.

the carboxylic esters. Hydrolysis of the esters afforded the desired products **17**−**20**.

Table 1 summarizes the in vitro PPARα, PPARγ, and PPARδ transactivation (TA)[7−9] EC_{50} data for new indole series of **2**−**16** synthesized. Rosiglitazone was used as PPARγ selective agonist control. The lead **1** previously reported by us containing a fibrate acid group attached to the 5-postion of indole and linked though a three-carbon linker to naphthophenone tail part showed a potent PPARα/γ dual agonist activity.[8] On the basis of our previous observation[7] and literature report[10] that a three-carbon linker between the aromatic head and tail part is appropriate for maintaining optimum activity levels, we retained the three-carbon linker with the indole head part and varied the tail part naphthophenone building block of **1** to get insight into the role

played by the tail part in providing potent PPAR agonist activity. Thus, changing the 2-naphthophenone tail part to 1-naphthophenone as in **2** led to a loss of potency for PPARγ receptor. Moving the benzoyl group from C-2 position to C-1 position of the naphthyl ring might disrupt the molecule from achieving a proper U-shaped structure for binding to the receptor which was observed in the X-ray cocrystal structure of indole series of compounds.[8]

Moreover, reduction of the carbonyl group in the tail part of **1** to methylene linker as in **3** led to a change in the sp^2 hybridized planar carbonyl function to sp^3 hybridized methylene group with a tetrahedral geometry, effecting a change in the relative positioning of naphthalene and phenyl ring of the tail part. This modification led to a complete loss of activity toward the PPAR receptor, which again shows that the orientation of the tail part building block is essential for maintaining the activity at PPAR receptor.

Since **2** and **3** showed loss of PPAR activation, we turned our attention to the phenyl ring in the naphthophenone moiety. Replacement of the terminal phenyl ring with a smaller methyl group as in **4** led to a decrease in activity that is more pronounced in PPARα than in the PPARγ receptor. Moreover, when the phenyl ring was replaced with a sterically equivalent 4-pyridyl ring (**5**), there was a loss of activity compared to **1**. However, replacement of the phenyl group with 3-furanyl group as in **6** retained the activity, showing that electronic factors might have major influence for PPAR activity. Consequently, this led us to retain the naphthophenone tail part building block of **1** and make changes by introducing electron-donating substituent "−OMe" and electron-withdrawing substituent "F" in the phenyl ring of the tail part. Subsequently, **8** with an electron-donating substitution was found to be as potent as **1** for PPARα/γ dual agonist activity, but the electron-withdrawing substitution in **7** led to loss of activity.

As the above modifications of naphthophenone did not result in improvement in PPAR activity, we switched the connectivity of the naphthophenone tail part to the linker by attaching the phenyl ring to the linker chain instead of the naphthyl ring; thus, **9** was found to have improved activity with a 2-fold better PPARγ activity and 4-fold better PPARα-selectivity when compared to **1**. Interestingly, when the fibrate acid group of **9** was moved from the 5-position to the 4-position of the indole head part, **10** showed potent and selective PPARα activation with more than 100-fold selectivity for the PPARα receptor over the PPARγ and PPARδ isoforms. Next, we applied the "benzosplitting"[11] concept to design two new compounds **11** and **12** with the 4-phenylbenzophenone tail part from **9** and **10**. It was found that the introduction of 4-phenylbenzophenone instead of the naphthophenone led to PPARγ selective activity in **11** and **12**. Introduction of 4-phenylbenzophenone instead of naphthophenone resulted in changing the molecule's PPAR subtype selectivity pattern, with a net result that PPARα/γ dual agonist **1** was converted to PPARγ selective agonist **11**. Both **11** and **12** with the novel 4-phenylbenzophenone tail part showed an order of selectivity toward PPARγ over PPARα receptor, with the 5-position isomer **11** being 5-fold more potent at PPARγ than the initial lead **1**. Compounds **11** and **12** displayed PPARγ selective agonist activity with a potency range similar to rosiglitazone; however, rosiglitazone was more selective to PPARγ than both compounds.

Intrigued by this switch in selectivity from dual PPARα/γ to PPARγ by varying the tail part, we explored the role of 4-phenyl moiety of the tail part 4-phenylbenzophenone scaffold. Thus, **13** and **14** were synthesized by replacing 4-phenyl group with 4-H and they were found to regain ∼100-fold PPARα activity compared to **11/12**. Compound **13**, where the fibrate acid group is attached to the 5-postion of the indole, showed potent dual PPARα/γ activity. However, moving the fibrate acid group to the 4-postion of the indole led to potent PPARα isoform selectivity in **12** similar to that observed in **10**. In this study **12** displayed maximum potency for PPARα (EC_{50} = 30 nM) with more than 300-fold selectivity over PPARγ/δ receptors. Next, replacement of the 4-phenyl moiety with an electron withdrawing 4-F or electron donating 4-OCH_3 substituent was done to give **15** or **16**, respectively. Both **15** and **16** showed dual PPARα/γ activation. In effect, **13**−**16** were dual PPARα/γ or PPARα selective compounds, clearly showing the importance of tail part 4-phenylbenzophenone scaffold in imparting selective PPARγ activity. The hydrophobic nature and the steric bulk of the 4-phenyl moiety in **11/12** might play an important role for selective interaction with the PPARγ receptor.

As replacement of the naphthophenone tail part of **1** with 4-phenylbenzophenone resulted in a shift from dual PPARα/γ to selective PPARγ activity in **11**, to get structural biology insight into the role played by 4-phenylbenzophenone tail part in imparting selective and potent PPARγ activity, the X-ray cocrystal complex of **11**-PPARγ was solved. The carboxylic acid of **11** conserved four H-bonds with Tyr473, His 449, His323, and Ser289. The H-bond interactions with these residues have been reported to stabilize the activation function helix (AF-2 helix) in PPARγ and consequently assist the recruitment of coactivators.[12] The indole ring of **11**, located around helixes 3, 5, 7, and 10, formed strong hydrophobic interactions with Tyr327, Leu330, and His449. The linker of **11** was close to the hydrophobic pocket of PPAR consisting of Leu330, Met334, Phe367, Val339, and Met364. The hydrophobic tail part of **11** and the propyl moiety occupied the region near the entrance of the binding pocket and had extensive interactions with the surrounding residues, including Cys285, I341, Met348, L255, and Glu259. Moreover, the fibrate moiety of **11** made close interactions with Phe282, Cys285, Gln286, and Ser289.

Comparison of the X-ray cocrystals of **1**, which has a naphthophenone tail part,[8] with **11** which has the 4-phenylbenzophenone tail part revealed that the carboxylic acid head, indole ring, and linker superimposed very well with each other (Figure 2a). The difference occurred in the tail parts where the 4-phenylbenzophenone tail of **11** extended deeper into the pocket entrance and made extensive hydrophobic interactions with the surrounding residues with more stable binding energy of −48.2 kcal/mol while the binding energy of **1** with the naphthophenone tail part was −28.3 kcal/mol as calculated by the program Insight II. Moreover, the propyl group of **11** moved closer to the active site and formed additional interactions with R288, S289, I326, and L330, which might also contribute to the improved potency of **11**, compared to **1**.

As the introduction of 4-phenylbenzophenone tail in **11** leads to a loss of PPARα activity compared to **1**, structural alignment of the **1**−PPARγ and **11**-PPARγ complexes with PPARα protein (PDB ID 1K7L) was done (Figure 1s in Supporting Information). It showed that the Gly284 in PPARγ, the residue close to the benzophenone moiety, is replaced by Cys 275 in PPARα. The more bulky side chain Cys275 in PPARα would cause a steric clash with the 4-phenylbenzophenone moiety of **11**. Cys275 is located at the entrance of the binding pocket, and the steric hindrance with **11** might, at least partially, limit the access to the binding pocket, which led to a decrease in PPARα activity of **11**, compared to **1**.

Having identified a novel 4-phenylbenzophenone tail part, which imparted PPARγ selective activity in indole series, we

were interested to know if this tail part could improve PPARγ selective activity in compounds where the indole head part would be replaced with other heterocyclic rings. Moreover, **11** and **12** were only ~15-fold more selective, while rosiglitazone was >45-fold more selective to PPARγ over PPARα receptor. Hence, to identify a potent and selective PPARγ agonist and to investigate the PPARγ selectivity potential of the novel tail part, we further carried out chemical exploration using 1,2,3,4-tetrahydroquinoline instead of indole as the aromatic head part. 1,2,3,4-Tetrahydroquinoline ring was selected because of easy synthetic derivatization and because it could be considered as the ring expanded form of indole ring.

Compounds **17** and **18** (Table 2), bearing the fibrate acid group at the 5- and 6-position of tetrahydroquinoline, respectively, and linked from the N-terminal through a three-carbon linker to the naphthophenone tail part, showed potent PPARα/γ dual activity similar to indole **1**. Compound **17** with the fibrate acid group at the 5-position showed better activity at α and γ receptors, compared to **18**. Also tetrahydroquinoline **17** was 6.5-fold more potent at PPARγ than indole **1**, showing that the replacement of indole with tetrahydroquinoline ring had led to enhancement of PPARγ potency. Next, we investigated the effect of replacing the naphthophenone ring with the novel 4-phenylbenzophenone tail part and retaining tetrahydroquinoline head part in **17/18**. Thus, **19** and **20** bearing the novel 4-phenylbenzophenone were synthesized. Compounds **19** and **20** with 5- and 6-position fibrate acidic headgroups, respectively, were found to show highly potent and PPARγ selective activity. Similar to the indole series **11/12**, introduction of 4-phenylbenzophenone tail part in tetrahydroquinoline series **19/20** had led to potent PPARγ selective activity, confirming that 4-phenylbenzophenone indeed imparted potent and PPARγ selective activity when incorporated as the tail part. Moreover, **19** was ~4-fold more potent than rosiglitazone at PPARγ, while ~80-fold more selective to PPARγ over the PPARα receptor, similar to rosiglitazone.

To further elucidate the improved potency and selectivity of **19**, the X-ray cocrystal complex of **19**−PPARγ was solved. Superimposition of **19** with **11** revealed that the 1,2,3,4-tetrahydroquinoline ring of **19** adopted a different conformation from the indole ring of **11** where both rings are coplanar but the tetrahydroquinoline ring of **19** was rotated 90.06° relative to the indole ring of **11** along the axis perpendicular to the plane of the ring. Therefore, the tetrahydroquinoline ring of **19** formed more extensive interactions with the surrounding residues, including Phe282, Cys285, Phe363, and Met364, which were absent in the structure of **11** (Figure 2b). The additional interactions of 1,2,3,4-tetrahydroquinoline ring would contribute to the improved potency of **19**. Apart from the different orientation of the head part tetrahydroquinoline ring and slight movement of the linker, the carboxylic acid head and the 4-phenylbenzophenone tail of **19** superimposed well with that of **11**.

Structural alignment of the PPARγ-**19** with PPARα protein (PDB ID 1K7L) showed that the bulkier side chain of Cys275 in PPARα (the corresponding residue Gly284 in PPARγ) would cause steric clash with the 4-phenylbenzophenone tail of **19**, which explains the PPARγ selective activity of this compound being similar to that of **11** with the same 4-phenylbenzophenone tail part (Figure 1s of Supporting Information).

In conclusion, through a series of structural modifications in the tail part of indole fibrates **1** identified earlier as PPARα/γ dual agonist, we discovered **11** and **12** as PPARγ selective agonists. Use of alternative tetrahydroquinoline fibrates led to the synthesis of **19** as a potent and selective PPARγ agonist with >4-fold better PPARγ activity than rosiglitazone, which is currently used for antidiabetes therapy. X-ray cocrystal

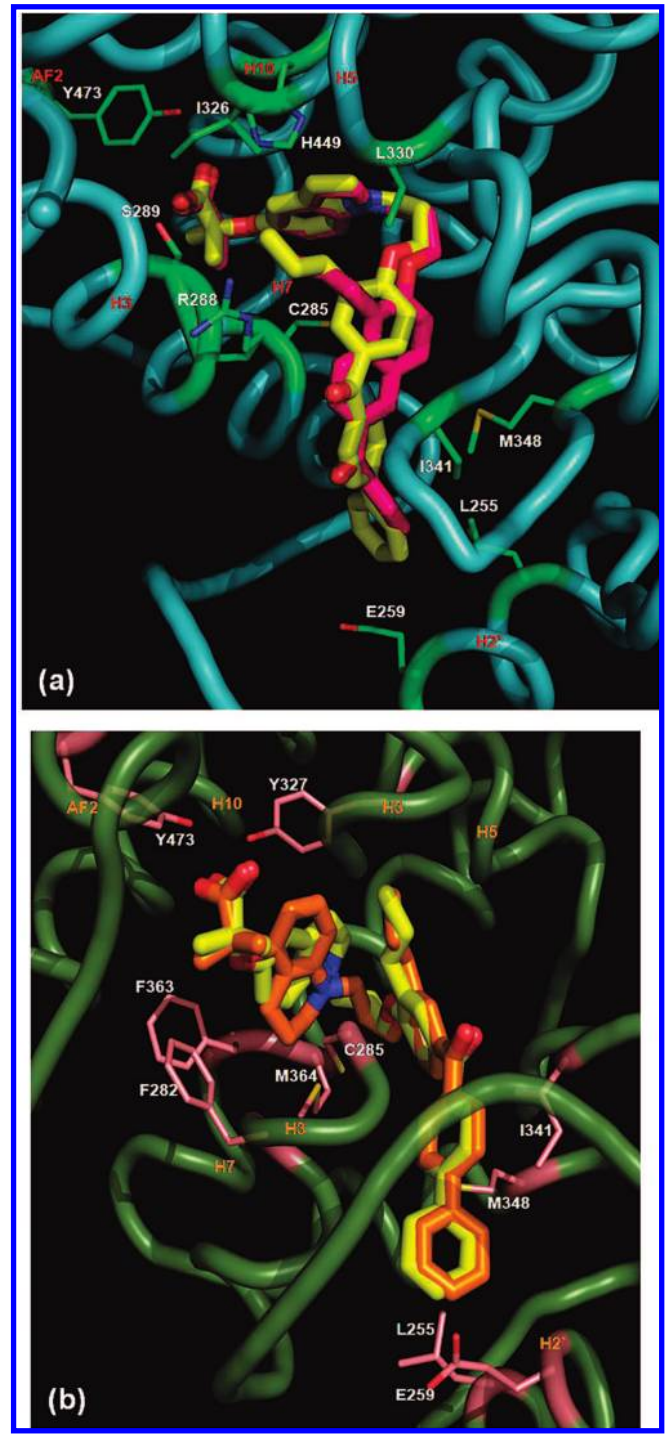

Figure 2. (a) Superposition of the X-ray structures of **1** (magenta) and **11** (yellow) in the binding pocket of PPARγ. The head parts of both compounds overlapped well, while the tail part building block 4-phenylbenzophenone of **11** extended deeper to the pocket entrance and made extensive hydrophobic interactions with the surrounding residues of PPARγ, explaining the improved PPARγ activity of **11** compared to **1**. (b) Superposition of the X-ray structures of **11** (yellow) and **19** (orange) in the binding pocket of PPARγ. Both compounds overlap well except for the head part aromatic rings. The tetrahydroquinoline ring of **19** is rotated 90.06° relative to the indole ring of **11** along the axis perpendicular to the plane of the ring and forms extensive hydrophobic interaction with the surrounding residues of PPARγ, explaining for the improved PPARγ activity of **19** compared to **11**. Key interacting residues are labeled.

Table 2. PPAR Agonist Activity of Tetrahydroquinoline Analogs **17**−**20**

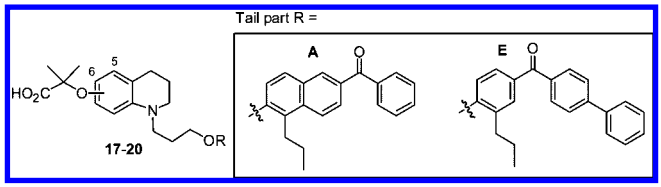

compd	quinoline position	tail part R	TA EC_{50} (μM)[a] α	γ	δ
17	5	A	0.12	0.1	>10
18	6	A	0.24	0.54	>10
19	5	E	3.99	0.05	>10
20	6	E	>10	0.10	>10
rosiglitazone			>10	0.22	>10

[a] Values are expressed as the mean of at least two independent determinations and are within ±15%.

analyses of **11** and **19** in complex with PPARγ reveal structural insight for the high degree of potency and selectivity observed with this novel tail part for the PPARγ isoform. Thus, focused SAR exploration led to the identification of the novel tail part building block 4-phenylbenzophenone, which confers selective PPARγ agonist activity when incorporated in the standard PPAR agonist design and could be useful in future endeavors to fine-tune PPAR isoform selectivity.

Experimental Section

2-(1-{3-[4-(Biphenyl-4-carbonyl)-2-propylphenoxy]propyl}-1,2,3,4-tetrahydroquinolin-5-yloxy)-2-methylpropionic Acid 19. A mixture of **25a** (0.20 g, 0.59 mmol), biphenyl-4-yl-(4-hydroxy-3-propylphenyl)methanone (tail part building block E) (0.15 g, 0.52 mmol), potassium carbonate (0.11 g, 0.78 mmol), and potassium iodide (0.01 g, 0.06 mmol) in 10 mL of DMF was heated at 120 °C for 2 h. The mixture was cooled to room temperature and quenched with water (10 mL) and was extracted with ethyl acetate (3 × 20 mL). The combined organic layer was washed with water (4 × 20 mL), followed by brine (2 × 20 mL), and then dried over anhydrous sodium sulfate. The solvent was removed in vacuo, the oily residue obtained was dissolved in a methanol and water mixture (4:1), 15 mL, LiOH (0.07 g, 1.77 mmol) was added, and the mixture was refluxed for 2 h. The solvent was removed in vacuo, and 0.5 N HCl was added to the residue and extracted with ether (3 × 20 mL). The combined organic layer was washed with water (2 × 20 mL), followed by brine (2 × 10 mL). The solvent was removed in vacuo, and the residue was chromatographed over a short column of silica gel, eluting with dichloromethane/methanol (98:2) to give **19** (0.18 g, 59%). ^{1}H NMR (400 MHz, $CDCl_3$) δ 1.00 (t, J = 7.6 Hz, 3H), 1.61 (s, 6H), 1.58 (m, 2H), 1.91−1.94 (m, 2H), 2.11−2.15 (m, 2H), 2.70 (t, J = 7.6, 2H), 3.27 (t, J = 5.6 Hz, 2H), 3.52 (t, J = 7.2, 2H), 4.12 (t, J = 5.6 Hz, 2H), 4.13 (t, J = 5.6 Hz, 2H), 6.17 (d, J = 7.6 Hz, 1H), 6.4 (d, J = 8.4 Hz, 2H), 6.88 (d, J = 8.8 Hz, 2H), 6.86−6.93 (m, 1H), 7.38−7.51 (m, 3H), 7.65−7.73 (m, 5H), 7.84−7.87 (m, 2H); ^{13}C NMR (100 MHz, $CDCl_3$) δ 14.1 (CH_3), 21.7 (CH_2), 22.1 (CH_2), 22.9 (CH_2), 25.1 (CH_3 × 2), 26.4 (CH_2), 32.4 (CH_2), 48.7 (CH_2), 49.3 (CH_2), 65.6 (CH_2), 80.4 (C), 105.8 (CH), 106.0 (CH), 110.0 (CH), 114.1 (C), 126.5 (CH), 126.8 (CH × 2), 127.3 (CH × 2), 128.1 (CH), 128.9 (CH), 129.8 (C), 130.4 (CH × 2), 130.5 (CH), 131.0 (C), 131.0 (C), 132.2 (CH), 137.1 (C), 140.1 (C), 144.6 (C), 146.6 (C), 152.5 (C), 160.4 (C), 176.2 (C), 195.5 (C); HRMS (EI) calcd for $C_{38}H_{41}NO_5$ (M^+) 591.2985, found 591.2980.

Compounds **2**−**18**, **20** were synthesized in a manner similar to that for **19**, using **21a**,**b**/**25a**,**b** and tail part building blocks **A**−**E**.

Acknowledgment. Financial support from National Health Research Institutes, Taiwan, National Science Council, Taiwan, and National Tsing Hua University, Taiwan, is gratefully acknowledged. We thank the staff of beamline BL13B1 and BL13C1 at National Synchrotron Radiation Research Centre (NSRRC), Taiwan, for technical assistance.

Supporting Information Available: Synthetic procedures; spectral data for tetrahydroquinoline head part **25a**,**b** and tail part building blocks **A**−**E**, **2**−**18**, **20**; HPLC purity of **9**, **11**, **12**, **14**, **19**, **20**; X-ray structure refinement for **11**−PPARγ and **19**−PPARγ (PDB ID 3GBK); structural alignment of **11** and **19** in PPARα binding pocket. This material is available free of charge via the Internet at http://pubs.acs.org.

References

(1) Reilly, M. P.; Rader, D. J. The metabolic syndrome: more than the sum of its parts. *Circulation* **2003**, *108*, 1546–1551.
(2) Diabetes: Diabetes Facts. http://www.who.int/mediacentre/factsheets/fs312/en/index.html, July 2008.
(3) Willson, T. M.; Brown, P. J.; Sternbach, D. D.; Henke, B. R. The PPARs: from orphan receptors to drug discovery. *J. Med. Chem.* **2000**, *43*, 527–550.
(4) Sarafidis, P. A. Thiazolidinedione derivatives in diabetes and cardiovascular disease: an update. *Fundam. Clin. Pharmacol.* **2008**, *22*, 247–264.
(5) Henke, B. R. Peroxisome proliferator-activated receptor alpha/gamma dual agonists for the treatment of type 2 diabetes. *J. Med. Chem.* **2004**, *47*, 4118–4127.
(6) Narkar, V. A.; Downes, M.; Yu, R. T.; Embler, E.; Wang, Y. X.; Banayo, E.; Mihaylova, M. M.; Nelson, M. C.; Zou, Y.; Juguilon, H.; Kang, H.; Shaw, R. J.; Evans, R. M. AMPK and PPARdelta agonists are exercise mimetics. *Cell* **2008**, *134*, 405–415.
(7) Mahindroo, N.; Huang, C. F.; Peng, Y. H.; Wang, C. C.; Liao, C. C.; Lien, T. W.; Chittimalla, S. K.; Huang, W. J.; Chai, C. H.; Prakash, E.; Chen, C. P.; Hsu, T. A.; Peng, C. H.; Lu, I. L.; Lee, L. H.; Chang, Y. W.; Chen, W. C.; Chou, Y. C.; Chen, C. T.; Goparaju, C. M.; Chen, Y. S.; Lan, S. J.; Yu, M. C.; Chen, X.; Chao, Y. S.; Wu, S. Y.; Hsieh, H. P. Novel indole-based peroxisome proliferator-activated receptor agonists: design, SAR, structural biology, and biological activities. *J. Med. Chem.* **2005**, *48*, 8194–8208.
(8) Mahindroo, N.; Peng, Y. H.; Lin, C. H.; Tan, U. K.; Prakash, E.; Lien, T. W.; Lu, I. L.; Lee, H. J.; Hsu, J. T.; Chen, X.; Liao, C. C.; Lyu, P. C.; Chao, Y. S.; Wu, S. Y.; Hsieh, H. P. Structural basis for the structure−activity relationships of peroxisome proliferator-activated receptor agonists. *J. Med. Chem.* **2006**, *49*, 6421–6424.
(9) Mahindroo, N.; Wang, C. C.; Liao, C. C.; Huang, C. F.; Lu, I. L.; Lien, T. W.; Peng, Y. H.; Huang, W. J.; Lin, Y. T.; Hsu, M. C.; Lin, C. H.; Tsai, C. H.; Hsu, J. T.; Chen, X.; Lyu, P. C.; Chao, Y. S.; Wu, S. Y.; Hsieh, H. P. Indol-1-yl acetic acids as peroxisome proliferator-activated receptor agonists: design, synthesis, structural biology, and molecular docking studies. *J. Med. Chem.* **2006**, *49*, 1212–1216.
(10) Desai, R. C.; Han, W.; Metzger, E. J.; Bergman, J. P.; Gratale, D. F.; MacNaul, K. L.; Berger, J. P.; Doebber, T. W.; Leung, K.; Moller, D. E.; Heck, J. V.; Sahoo, S. P. 5-Aryl thiazolidine-2,4-diones: discovery of PPAR dual alpha/gamma agonists as antidiabetic agents. *Bioorg. Med. Chem. Lett.* **2003**, *13*, 2795–2798.
(11) Wermuth, C. G. Application Strategies for Primary Structure−Activity Relationship Exploration. In *The Practice of Medicinal Chemistry*, 2nd ed.; Wermuth, C. G., Ed.; Academic Press: Boston, MA, 2003; pp 289−300.
(12) Nolte, R. T.; Wisely, G. B.; Westin, S.; Cobb, J. E.; Lambert, M. H.; Kurokawa, R.; Rosenfeld, M. G.; Willson, T. M.; Glass, C. K.; Milburn, M. V. Ligand binding and co-activator assembly of the peroxisome proliferator-activated receptor-gamma. *Nature* **1998**, *395*, 137–143.

JM801594X